MICONIC:
The impact of AGN feedback on the nuclear multiphase ISM of Centaurus A

Lara Pantoni
(Postdoc - UGent)

On behalf of the MIRI nearby galaxy GTO team
Maarten Baes (Ghent), Almudena Alonso Herrero (Madrid), Pierre Guillard (Paris), Paul van der Werf (Leiden), Torsten Böker (Baltimore), Gillian Wright (PI MIRI UK ACT)...

This talk is based on the following publications:
- Pantoni et al. (2026); doi 10.48550/arXiv.2603.23674
- Alonso Herrero et al. (2025); doi 10.1051/0004-6361/202554823
- Evangelista et al. (2026); submitted to A&A

GHENT UNIVERSITY

MIRI European Consortium

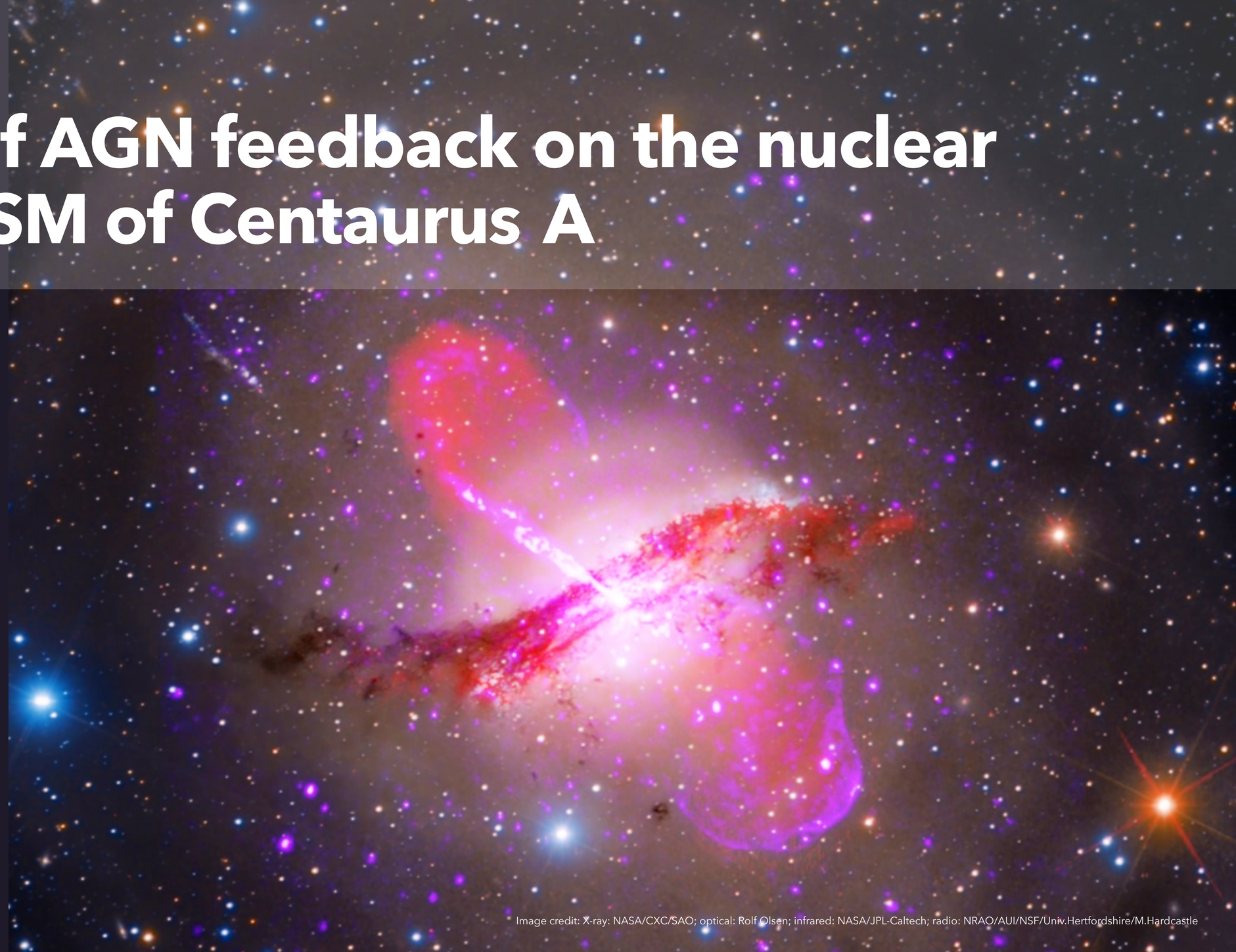

Image credit: X-ray: NASA/CXC/SAO; optical: Rolf Olsen; infrared: NASA/JPL-Caltech; radio: NRAO/AUI/NSF/Univ.Hertfordshire/M.Hardcastle

Cen A: ideal laboratory for AGN feedback

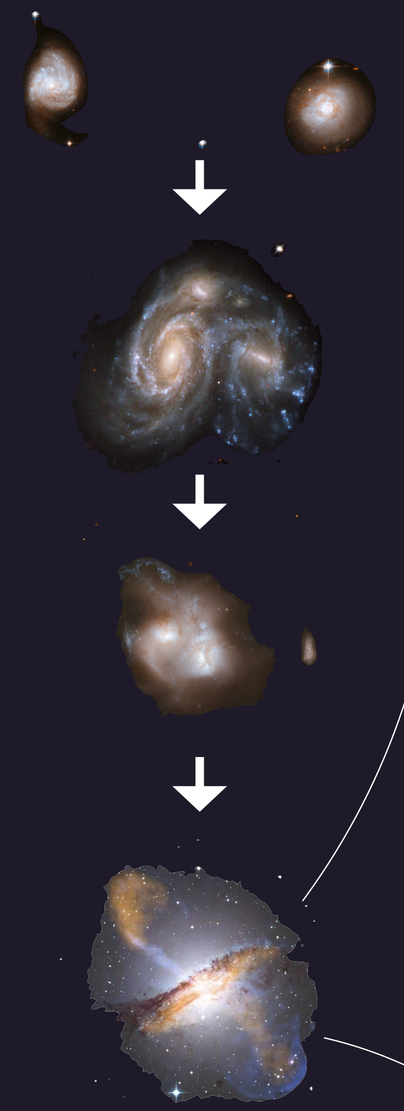

Galaxy **mergers** represent a critical and complex phase in galaxy evolution, often triggering intense episodes of **star formation** and **nuclear activity** that can profoundly **influence the subsequent evolution of the system**.

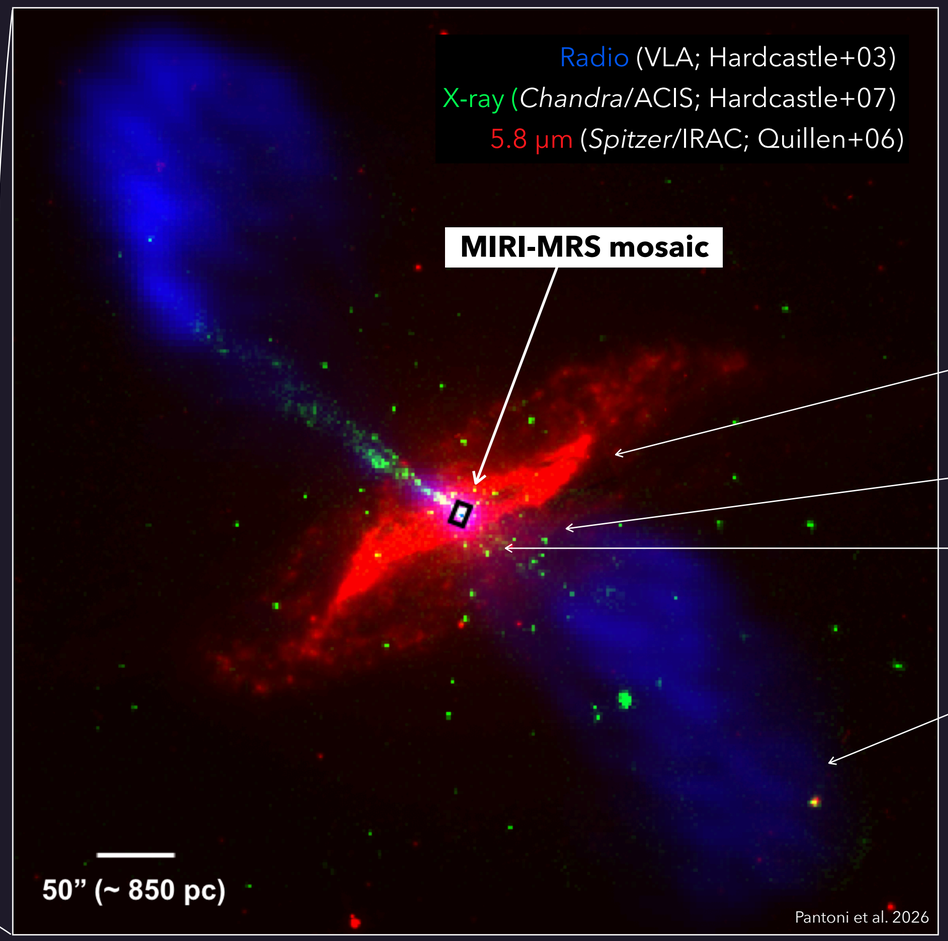

- ★ **RA** 13h 25m 27.615s
- ★ **DEC** -43° 01’ 08.805”
- ★ D ~ 3.5 Mpc (z = 0.001825) with **17 pc/”**
- ★ NCG 5128 (giant elliptical, peculiar)
- ★ Radio-loud AGN with relativistic jets

Warped molecular disk and **dust lane**, seen as a "parallelogram" or S-shaped structure in projection, sites of active SF.

Extended **shell** structures.

Inner jet close to the nucleus with a large inclination to the line-of-sight (~ 70°).

Giant radio lobes which extend up to 10° on the sky.

- Being the nearest active radio galaxy and the fifth brightest galaxy in the sky, Cen A is an ideal target to study the effect of AGN feedback on the nuclear ISM with JWST.

Image credits. Top three: NASA, ESA, the Hubble Heritage Team (STScI/AURA)-ESA/Hubble Collaboration and A. Evans (University of Virginia, Charlottesville/NRAO/Stony Brook University), K. Noll (STScI), and J. Westphal (Caltech); bottom: X-ray: NASA/CXC/CfA/R.Kraft et al.; Submillimeter: MPIfR/ESO/APEX/A.Weiss et al.; Optical: ESO/WFI

MICONIC: MIRI-MRS observations of Cen A's center

★ MICONIC is a **GTO program** of the **MIRI European Consortium** targeting the **(circum)nuclear region** of six nearby *iconic* centers, including **Cen A**.

★ It consists in ~30 hours of **MIRI/MRS 5-28μm** IFU spectroscopy and in coordination with the NIRSpec science team.

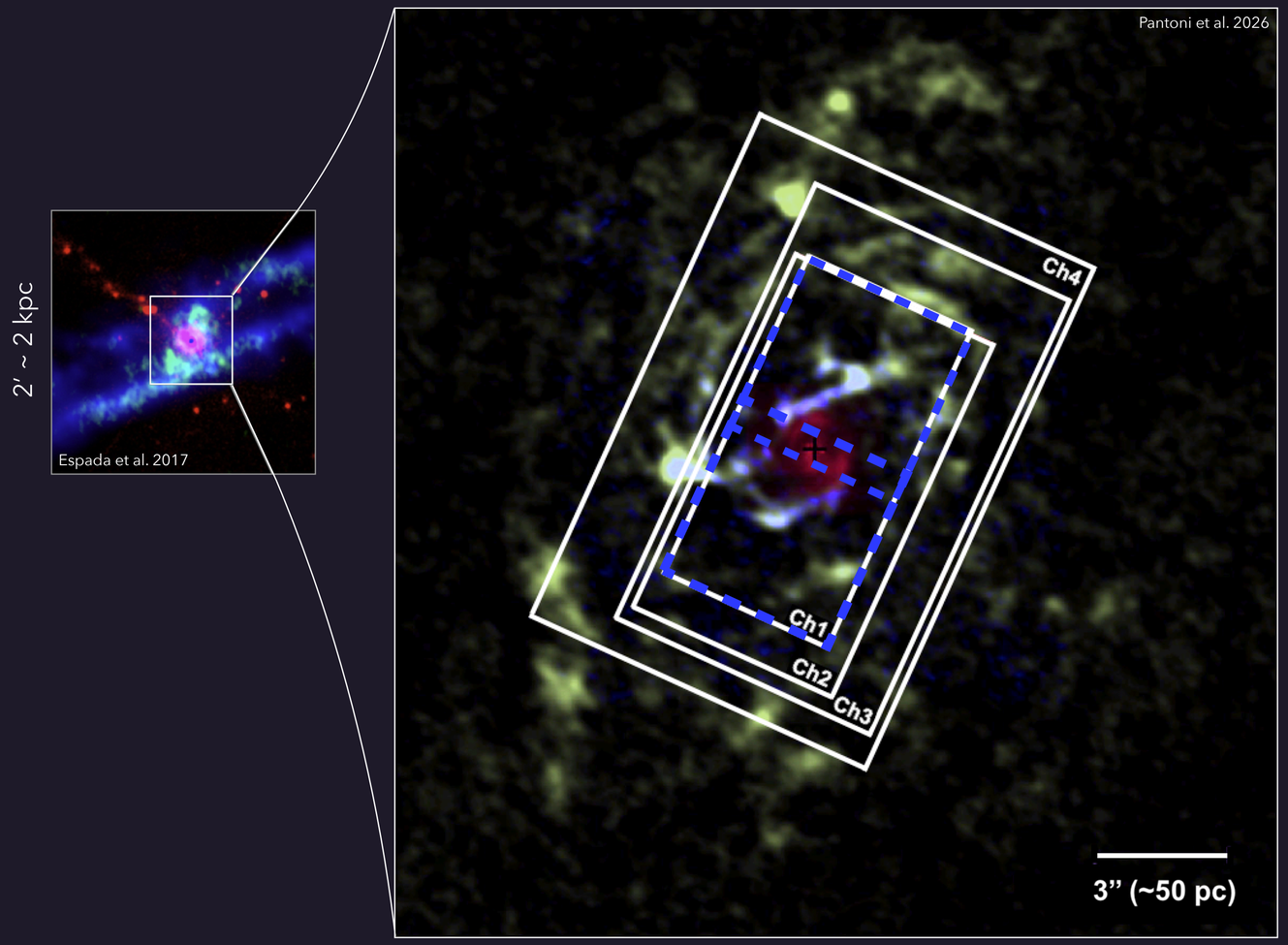

- JWST Cycle 1's GTO program ID 1269
- **1 × 2 mosaic** centred on the nucleus of Cen A, approximately **7" × 12"**, corresponding to a physical scale of ~ **100 pc × 200 pc**.
- Four integral field units ("channels"), with angular resolution in the range **0.3"-1" (5-17 pc)**.
- The full MRS spectral range was covered in a total of **1800 seconds** of on-source integration time.

Observations employed the 4-point dither pattern optimized for extended sources, with 10 groups per integration and 5 integrations per exposure, in FASTR1 readout mode.

MIRI-MRS spectrum of Cen A's centre

The MIRI-MRS spectrum of Cen A's centre reveals a rich set of **ionized gas emission lines** and the **H_2 0-0 S(1)–S(8)** transitions and prominent **PAH emission features** at 6.2, 7.7, 8.6, 11.2, 12.0, and 16.5 μm.

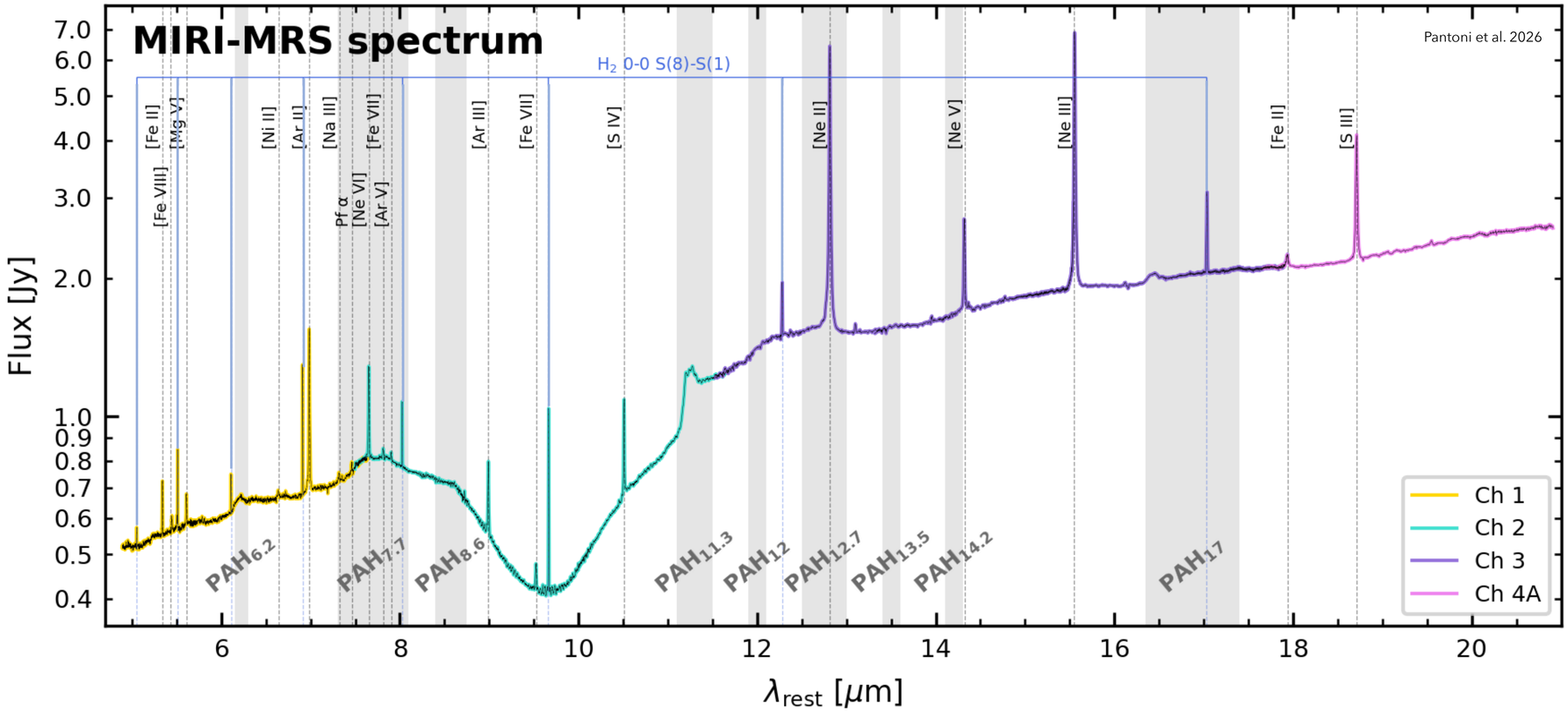

- Ionized gas and warm H_2 **kinematics** (Alonso-Herrero+25, A&A).
- Warm H_2 properties and **excitation mechanism** (Evangelista+26, submit.).
- Characterization of the **PAH features** (Pantoni+26, A&A).

Morphology and kinematics: ionized gas

We detect a large number of fine-structure lines.

Line	λ_{rest}	IP	flux	$FWHM_{line}$	ϵ
[Fe II]	5.340	7.9	4.84 ± 0.11	445	0.9
[Ar II]	6.985	15.8	49.55 ± 0.97	608	5.7
Pfα	7.460	...	1.08 ± 0.11	552	1.3
[Ne VI]	7.652	126.2	16.13 ± 0.39	397	3.8
[S IV]	10.511	34.8	8.25 ± 0.20	335	1.3
[Ne II]	12.814	21.6	156.45 ± 4.89	539	6.5
[Ne V]	14.322	97.1	19.80 ± 0.47	316	2.0
[Ne III]	15.555	41.0	110.78 ± 2.80	396	37.5
[S III]	18.713	23.3	33.39 ± 0.88	367	3.5
[Ne V]	24.318	97.1	18.72 ± 0.28	286	1.4
[O IV]	25.890	54.9	73.88 ± 1.33	307	1.8

The brightest are:

The broadest components …

…have **FWHM ~1425-1650 km/s** (see also Marconcini et al. 2025), likely associated with an **outflow** driven by the jet and/or the AGN.

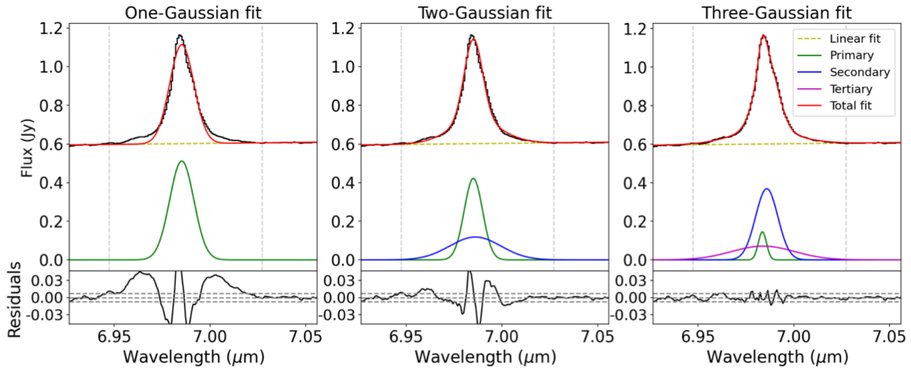

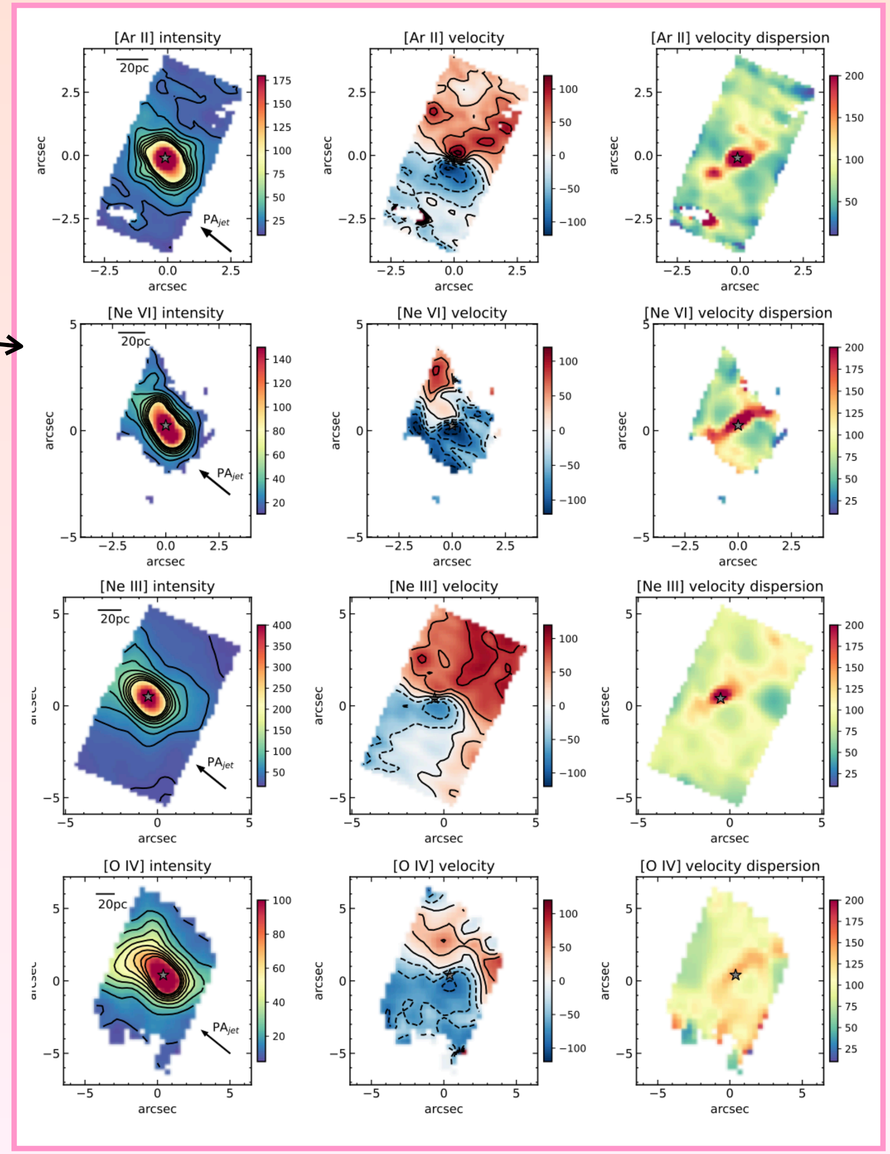

Alonso Herrero et al. (2025); doi 10.1051/0004-6361/202554823

Morphology and kinematics: ionized gas

Alonso Herrero et al. (2025); doi 10.1051/0004-6361/202554823

High IP line:

[O IV]

Ionization-cone-like morphology

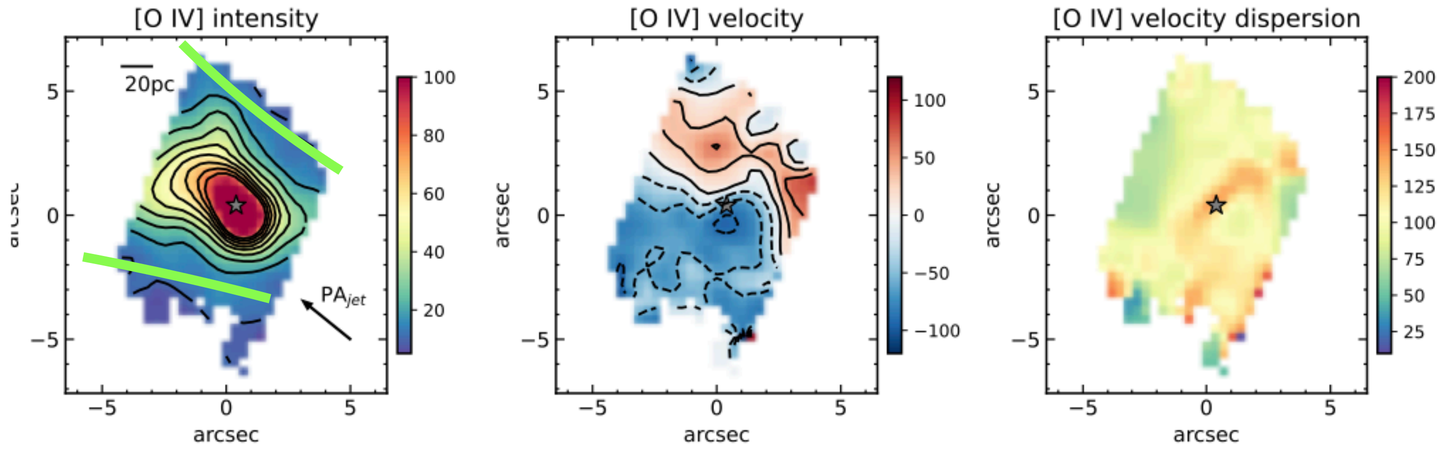

Low IP line:

[Ar II]

Emission also in the galaxy disk

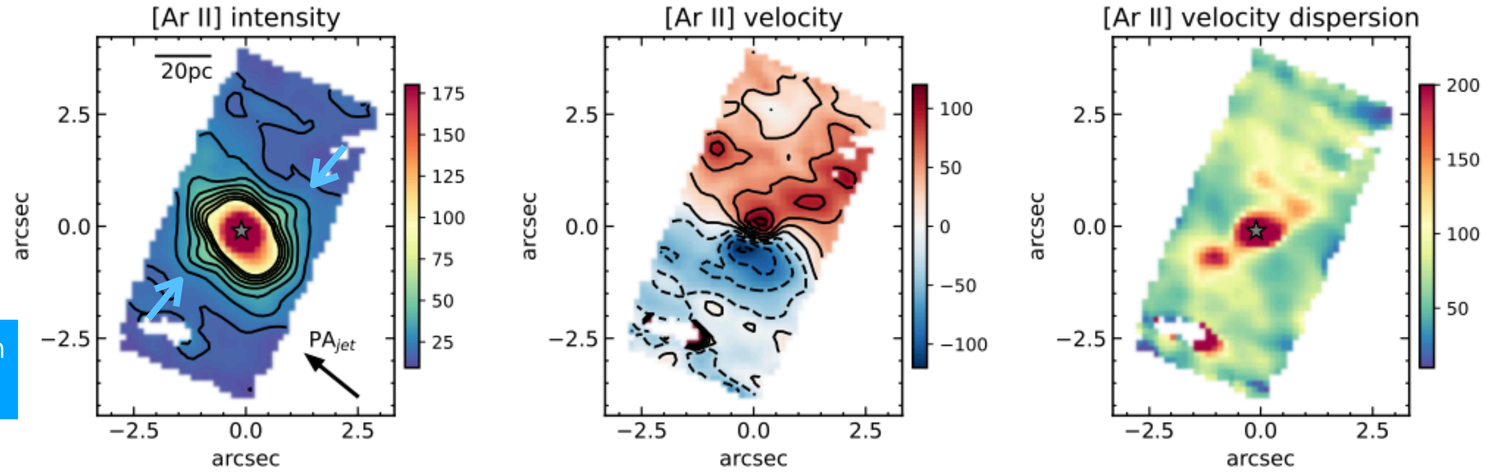

- the **mean-velocity fields** display **rotational motions** as well as **strong deviations from rotation**;
- **velocity dispersion** peaks at the **AGN location** and is larger in the direction **perpendicular to the jet**.

Morphology and kinematics: ionized gas

Alonso Herrero et al. (2025); doi 10.1051/0004-6361/202554823

Low IP line:

[Ar II]

Emission also in the galaxy disk

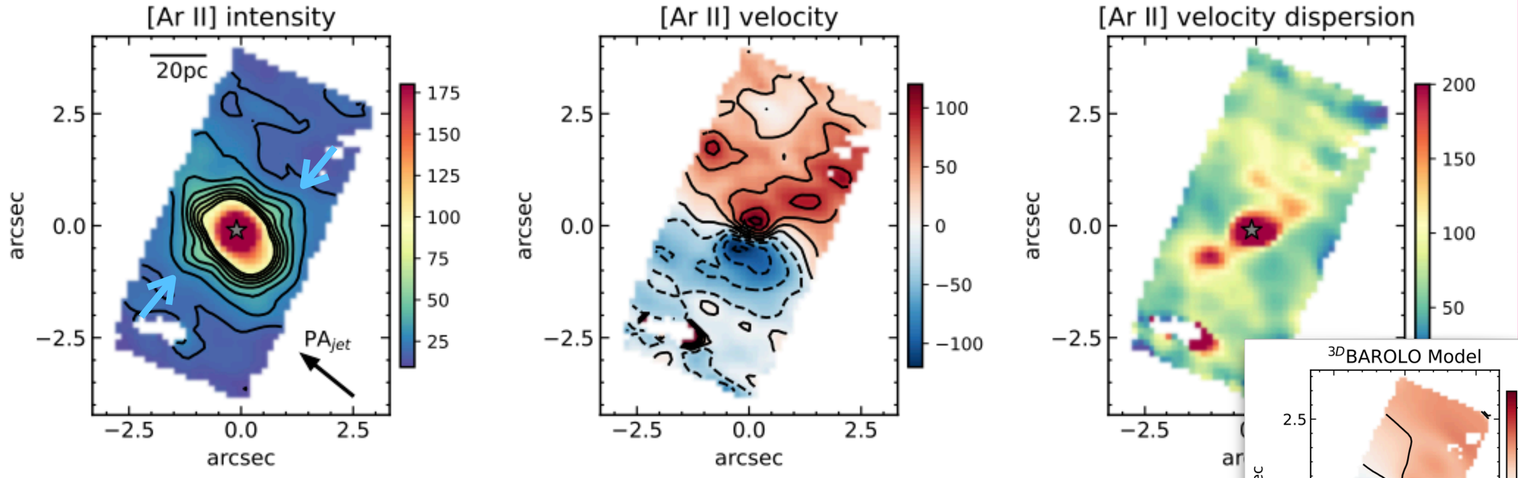

A fit with **3D BAROLO** (Di Teodoro & Fraternali 2015) gives…

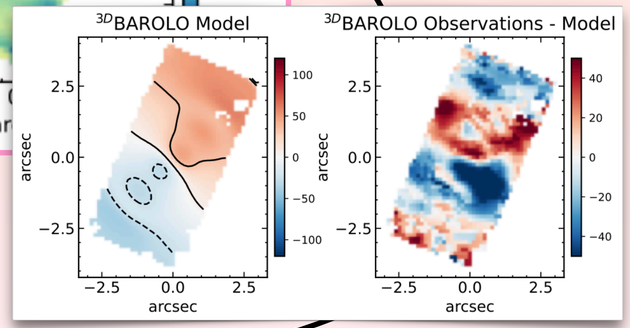

P-V diagrams

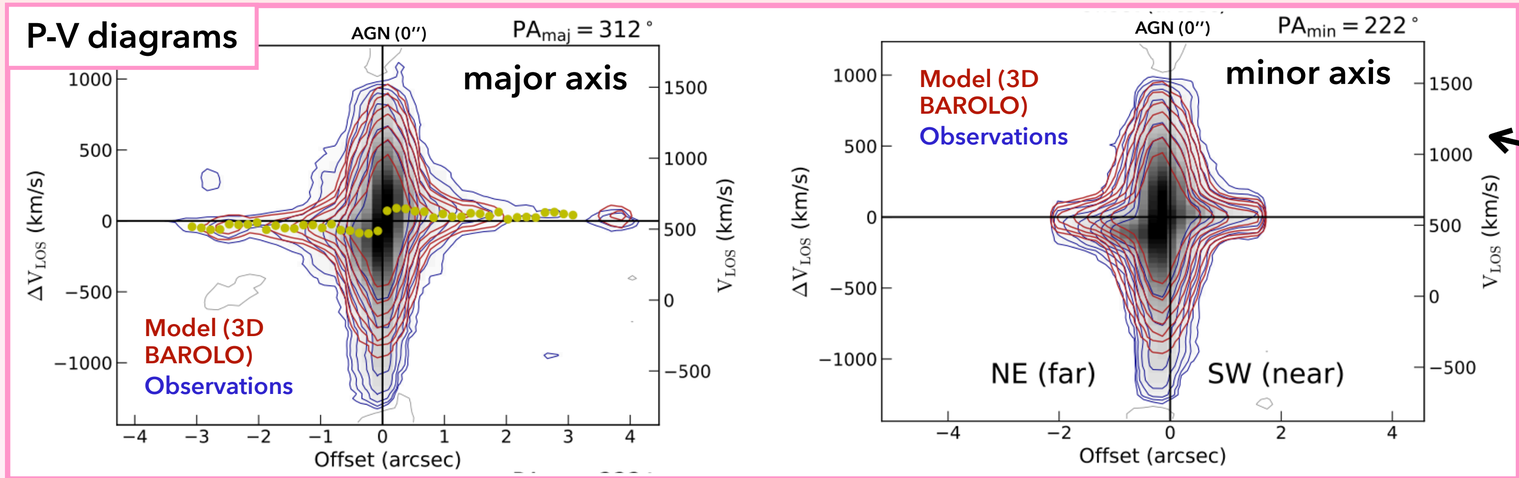

- At the AGN position the ionized gas reaches **v ~ 1000 km/s** and **−1400 km/s** along both kinematic axes.
- These high v are associated with the unresolved second (**broad**) gaussian **component**.
- Along the kinematic major axis at **r > 2''**, **the gas rotates** (low velocity dispersions).

Morphology and kinematics: warm H_2

Alonso Herrero et al. (2025); doi 10.1051/0004-6361/202554823

A fit with **3D BAROLO** (Di Teodoro & Fraternali 2015) gives…

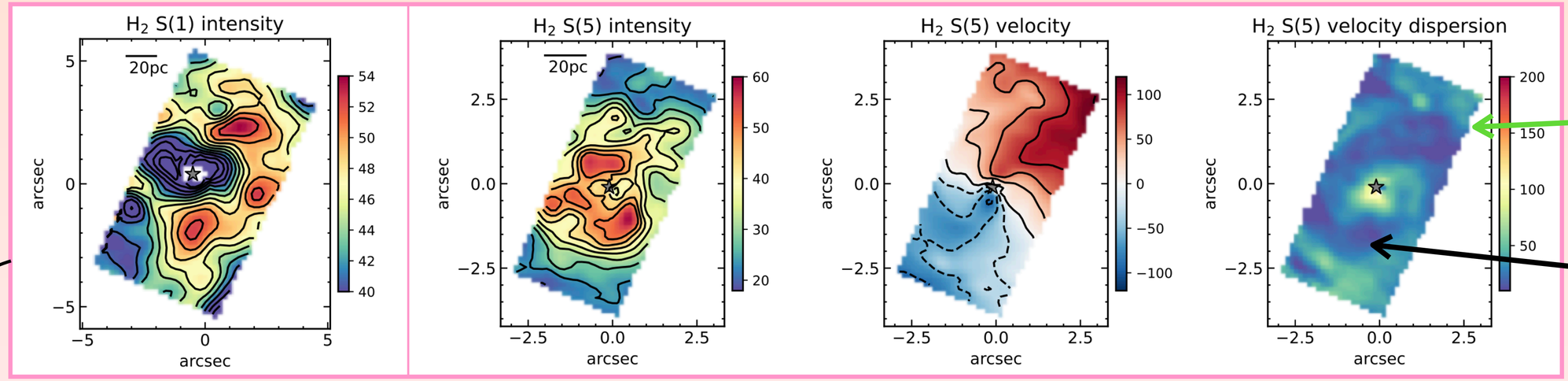

spiral-like morphology

instrument spectral resolution ~ 35 km/s

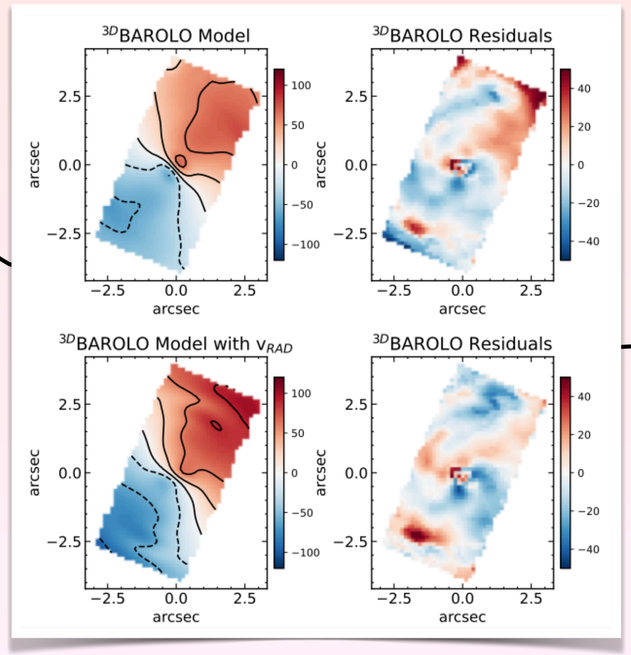

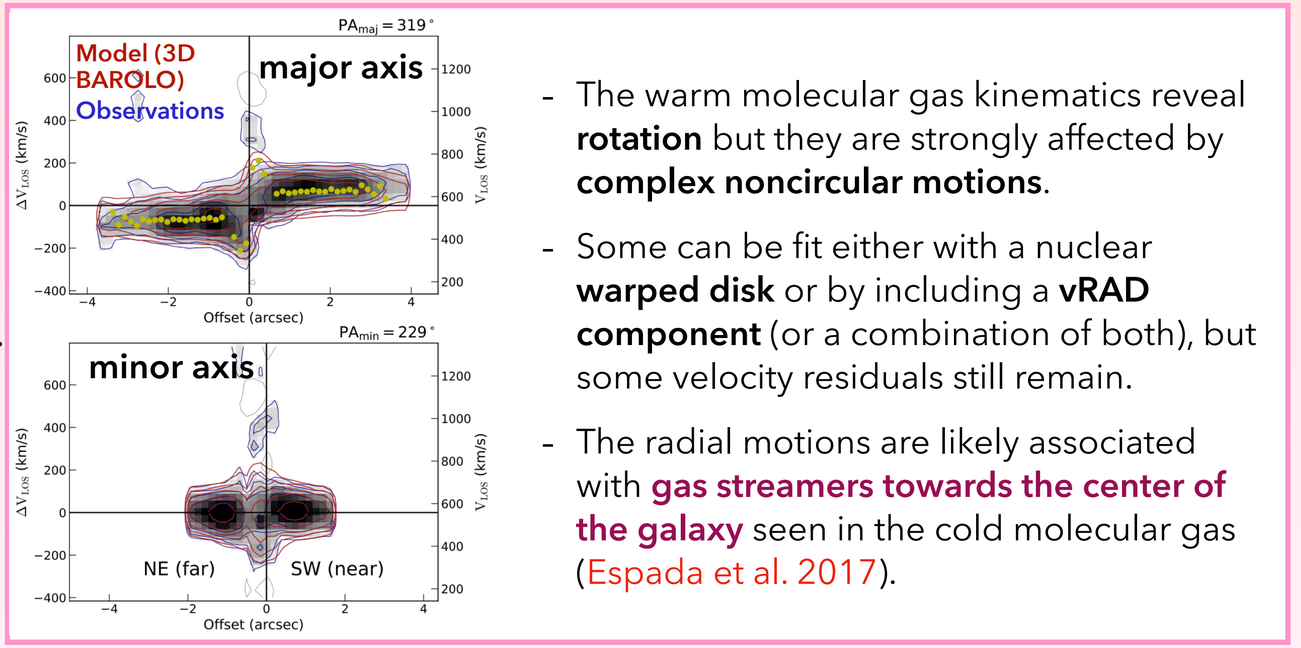

- The warm molecular gas kinematics reveal **rotation** but they are strongly affected by **complex noncircular motions**.
- Some can be fit either with a nuclear **warped disk** or by including a **vRAD component** (or a combination of both), but some velocity residuals still remain.
- The radial motions are likely associated with **gas streamers towards the center of the galaxy** seen in the cold molecular gas (Espada et al. 2017).

Excitation/ionization mechanisms: shocks?

Ionized gas

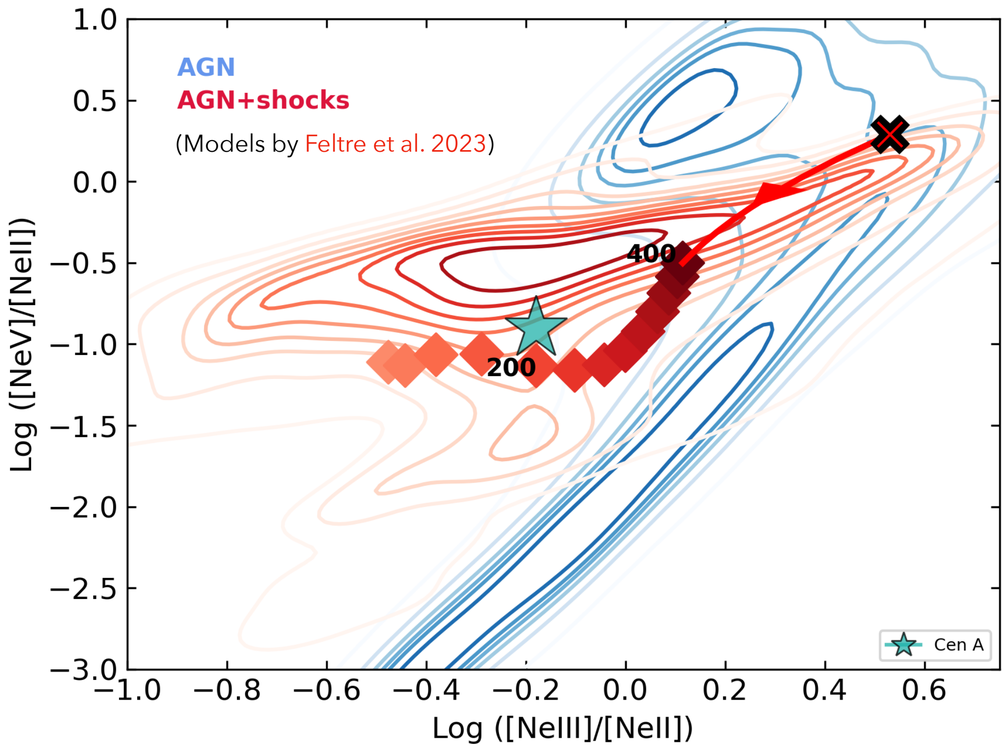

Pantoni et al. (2026); doi 10.48550/arXiv.2603.23674
Alonso Herrero et al. (2025); doi 10.1051/0004-6361/202554823

➡ Both **shocks** and **AGN photoionization** contribute to the gas ionization in the nuclear region and along the jet direction of Cen A in the inner ~100 pc.

Warm H_2

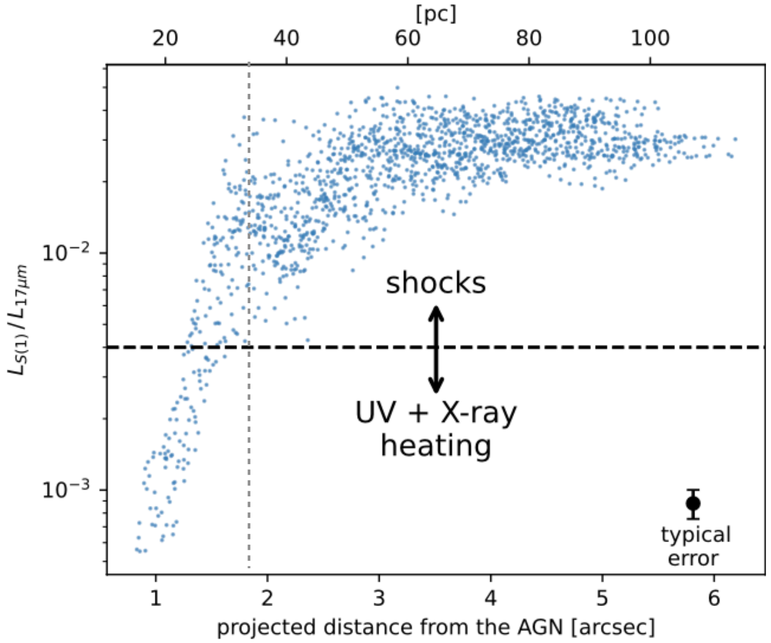

Spaxel-by-spaxel ratio of **H_2 0-0 S(1) luminosity** and **monochromatic continuum luminosity** at **17 μm.**

Rescaled excitation limit from Guillard et al. (2012b)

Evangelista et al. (2026); submitted to A&A

- $L_{H_2}/L_{17\mu m}$ **exceeds** the **PDR threshold**, indicating collisional excitation.
- $L_{H_2}/L_{X(2-10\,keV)}$ **exceeds** by a factor 4 the **XDR models**' upper limit.
- Dissipation of mechanical energy contributes to the excitation along the coherent spiral streamer.

➡ **shocks play an important role in heating H_2 and in causing loss of angular momentum** (see also Espada et al. 2017; Ogle et al. 2010)

PAHs in Cen A's center

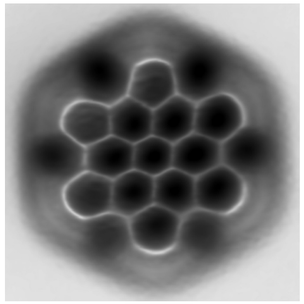

Hexabenzocoronene
Atomic Force Microscope image, black and white (CNRS, Toulouse, France).

Polycyclic Aromatic Hydrocarbons (**PAHs**):

- are compact, planar, carbon-based molecules composed of fused aromatic rings and typically containing between 20 and 500 carbon atoms (up to a few nm in size).
- are ubiquitous across the Universe, with detections out to redshift $z \sim 4$ (Riechers et al. 2014; Spilker et al. 2023).
- play a crucial role in the physics of the interstellar medium (heating and cooling, formation of H2, extinction of stellar light, obscured SF tracer; e.g., Tielens 2008).

➡ Do PAHs **survive** in the vicinity of **AGNs**? If yes, what are their **properties**? Do the AGN **alter** their **structure**?

PAHs in Cen A's center

PAH spatial distribution (mom0)

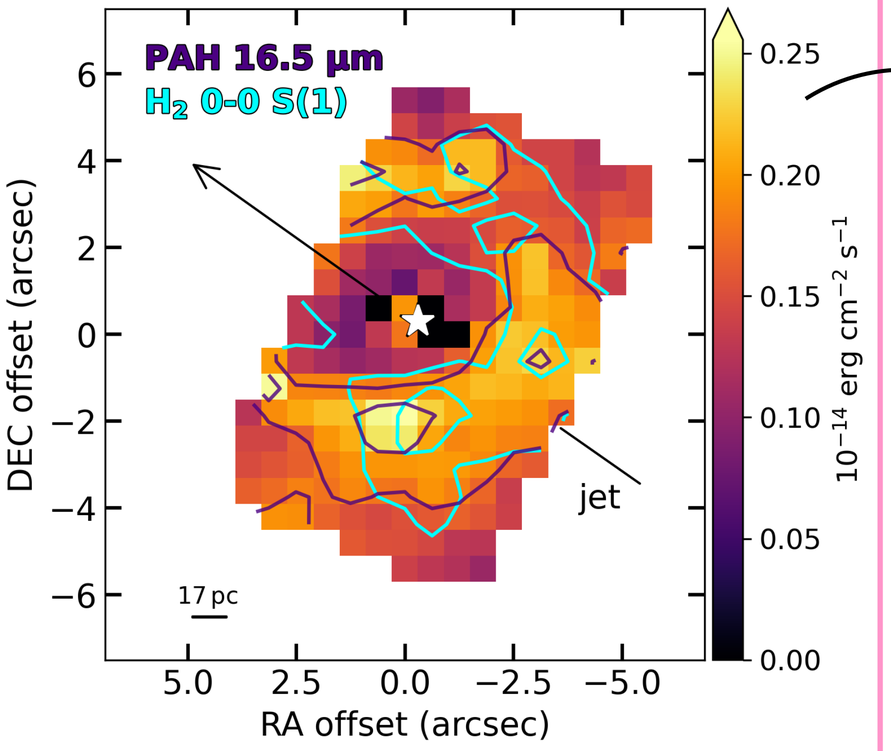

We identify some regions of interest in the mom0 map…

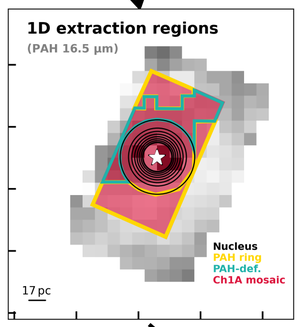

A fit with **SPIRIT** (Donnan et al. 2024) gives…

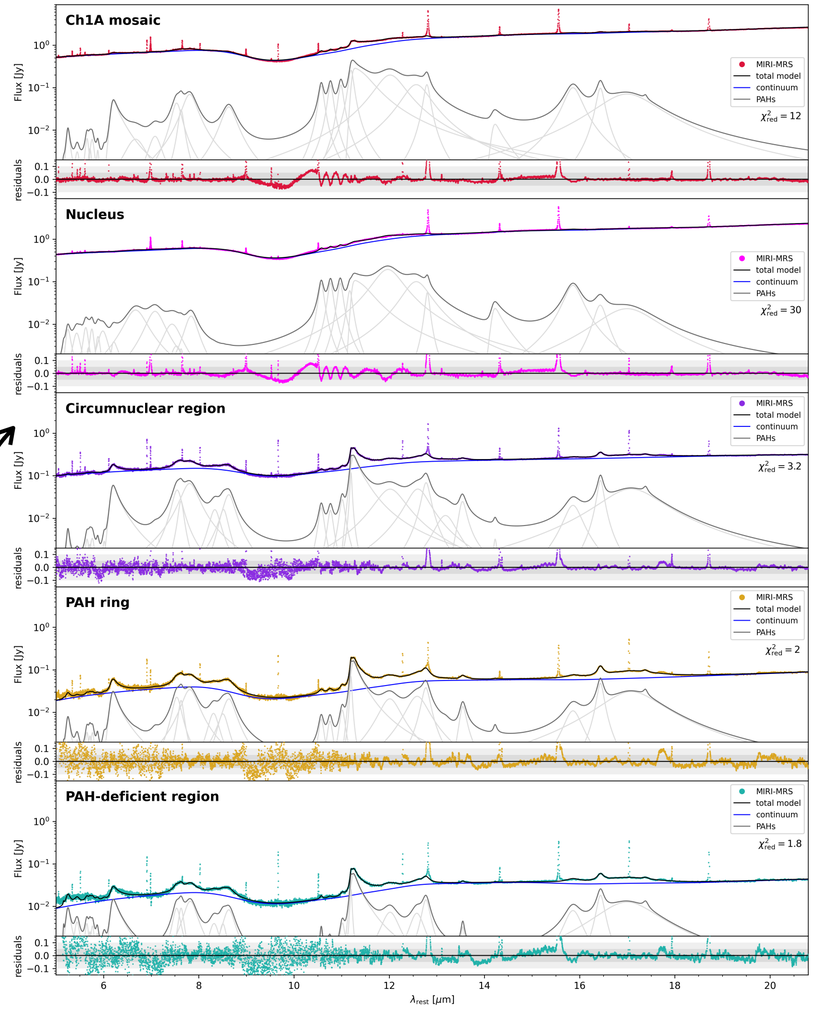

PAH fluxes and Equivalent widths

PAHs in Cen A's center

Because individual PAH bands arise from distinct vibrational modes, **PAH intensity ratios** provide powerful diagnostics of PAH **size**, **charge state**, and **molecular structure** (e.g. Draine & Li 2001; Galliano et al. 2008; Rigopoulou et al. 2021, 2024).

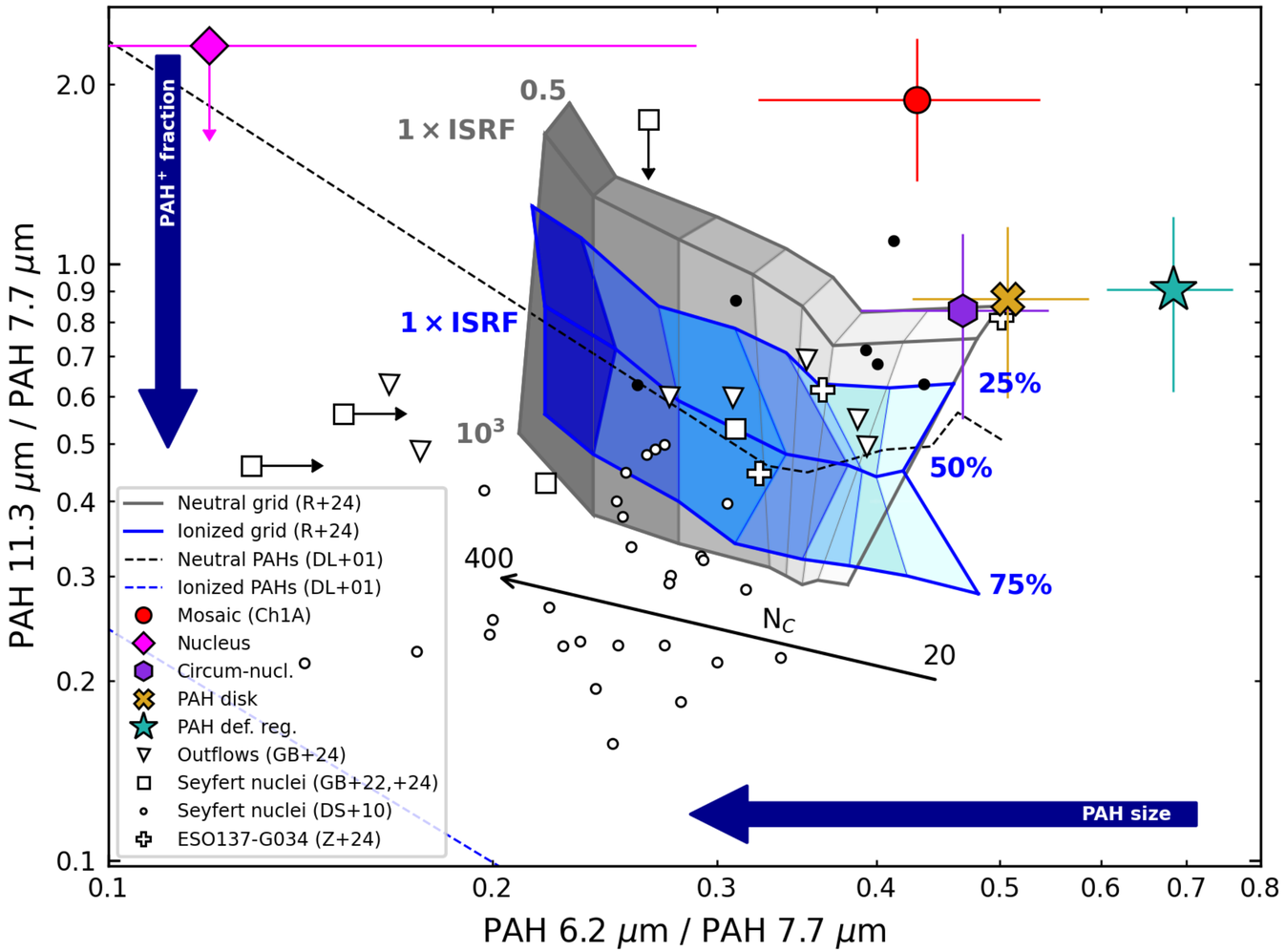

- **SHOCKS:**
  collisional excitation of H_2 (high H_2/PAH)

Extreme ratios in favor of (small) neutral PAHs.

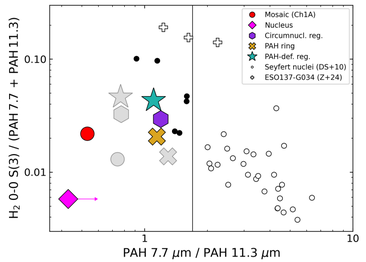

These extreme ratios can be naturally explained if the PAH population is dominated by **more open** and **irregular species**: i.e. **catacondensed PAHs**.

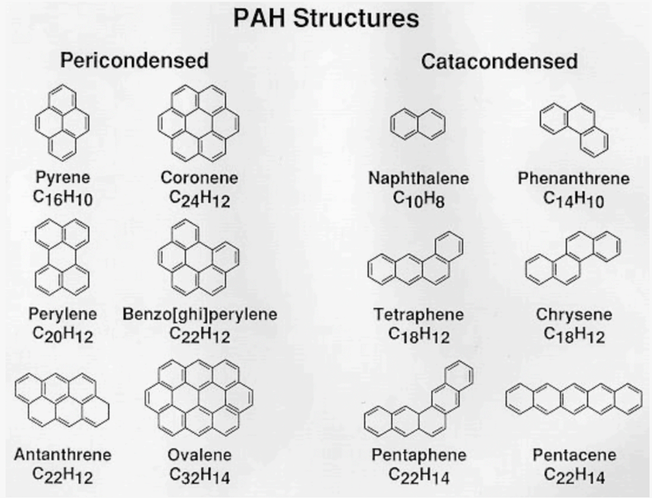

Salama et al. (1996)

PAHs in Cen A's center

PAH hydrogenation

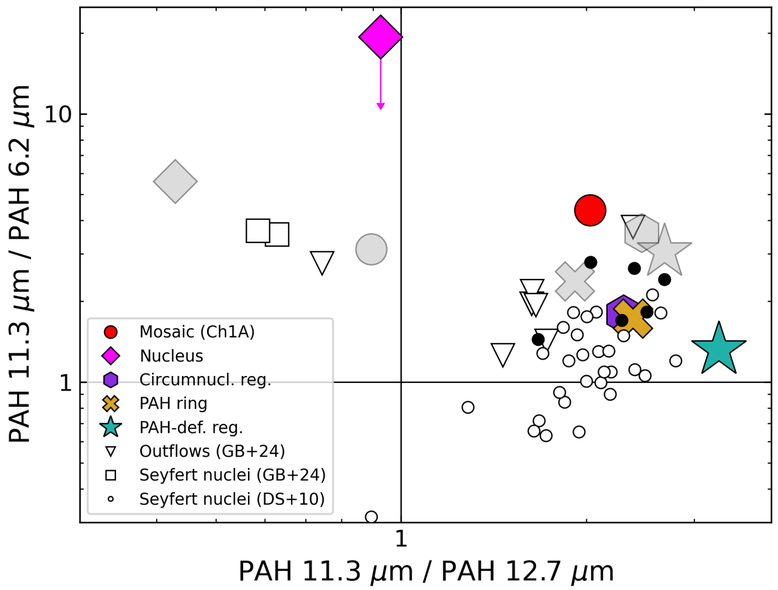

- Dominance of **solo** over duo or trio **hydrogen sites**.
- The most extreme case occurs in the **PAH-deficient region**, where we measured the **lowest** 11.3/12.7 ratio.

PAH equivalent widths

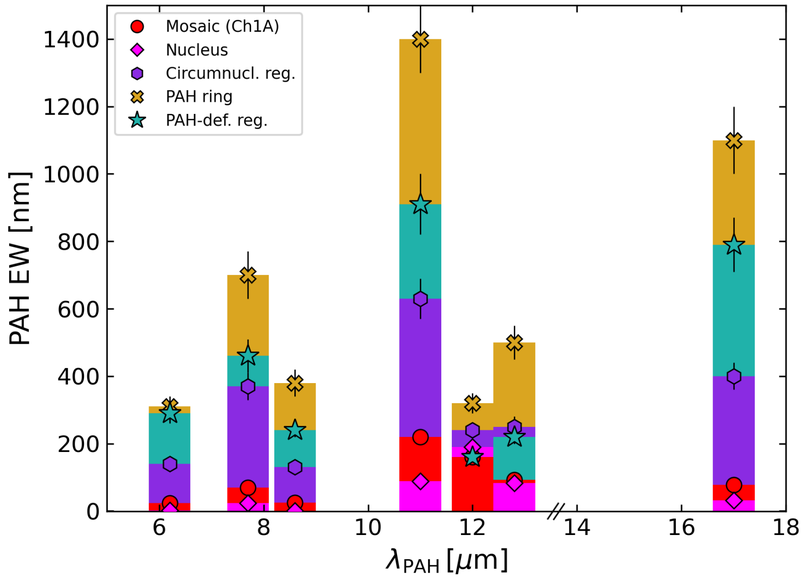

- Low PAH EWs in the full mosaic, the nucleus and circumnucl. region are mainly driven by AGN **continuum dilution**.
- **Largest** EWs in the PAH ring, and a **marked decrease** in the PAH-deficient region.

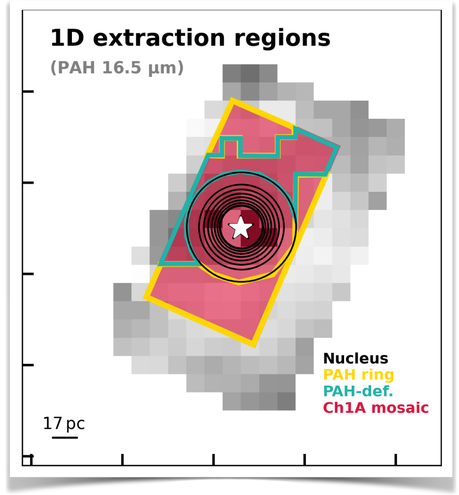

➡ Shocks may cause erosion or destruction of PAHs, as for the PAH- deficient region.

Summary

Evangelista et al. (2026); submitted to A&A
Pantoni et al. (2026); doi 10.48550/arXiv.2603.23674

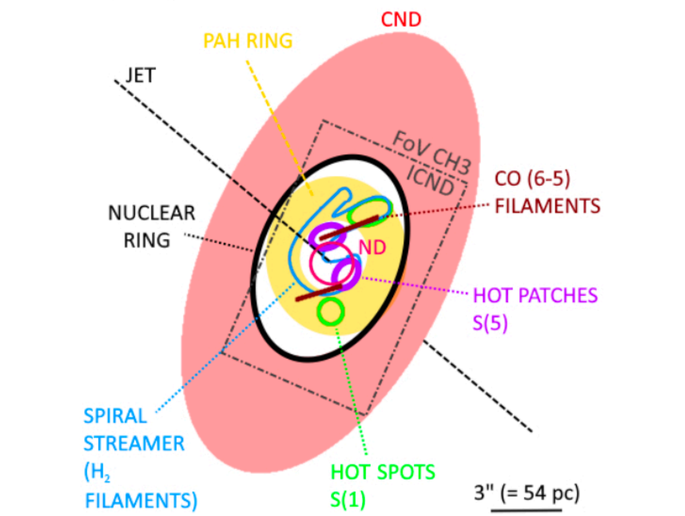

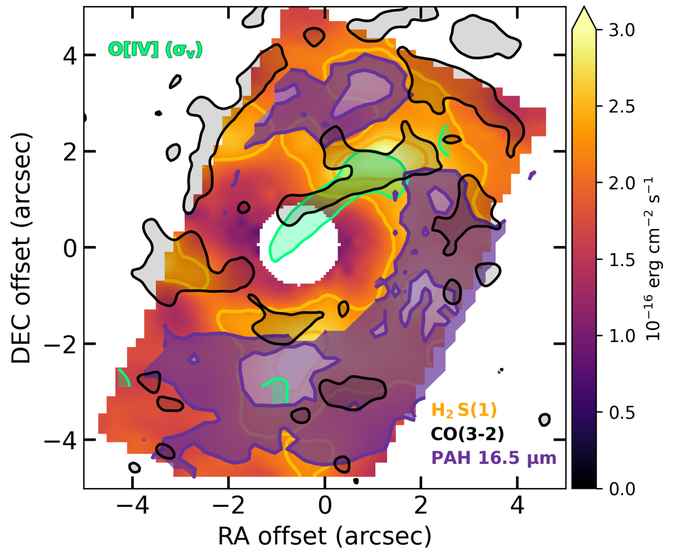

In this talk I have discussed the impact of the AGN and the radio jet on the properties of the multi-phase ISM in the inner 100-200 pc of Cen A, as observed by JWST MIRI-MRS:

IONIZED GAS

- Fast velocities in the ionized gas (~ 1000; -1400 km/s) are confined in the nuclear region (~ 6 pc).
- Velocities of hundreds km/s up to r ~ 40-50 pc are observational signature of the presence of a **jet-inflated bubble/outflow** in the central region.

WARM MOLECULAR HYDROGEN

- H_2 velocity maps show **global rotation** plus a **warped-disk geometry** and **non-circular motions**. The filaments display lower dispersion, consistent with a coherent inflow toward the AGN.
- Evidence of non-negligible **shock-heating** of H_2 and ionized gas.

PAHs

- PAH intensity ratios across the Cen A MIRI-MRS mosaic point to a strongly **reprocessed PAH population** dominated by **neutral species** with **solo hydrogen sites**, potentially exhibiting open and irregular structures (**catacondensed**).
- Shocks may cause erosion or destruction of PAHs (as for the PAH-deficient region); PAHs in the ring may be protected by large column density of the cold molecular gas (~10^22 cm-2; Israel et al. 2014).

Backup slides

Backup slides

Alonso Herrero et al. (2025); doi 10.1051/0004-6361/202554823

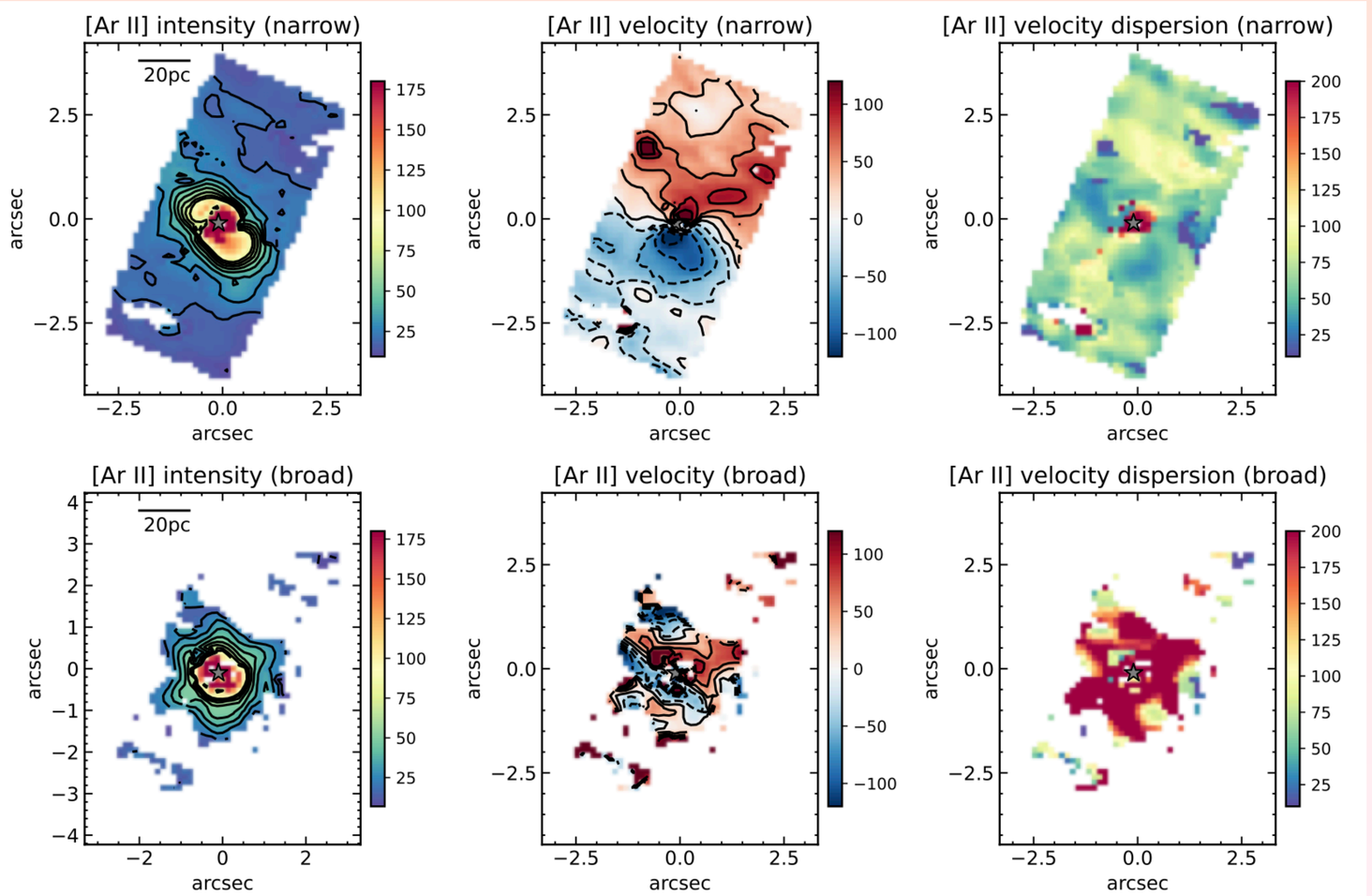

Fig. A.4. Same as Fig. 6 but for fits with two Gaussian components for the [Ar II] line. All velocities are referred to v_{sys}.

Backup slides

Excitation diagrams indicate that the average temperatures of the bulk of the H2 are almost ~2 times higher in the nucleus (416±12) K than in the ICND (286±7) K. The physical parameter maps show temperatures up to 340 K on the eastern ICND side, where the jet is pointed towards us. The filaments contain830 most of the molecular mass and show the lowest ortho-to-para ratio (~ 1.8).

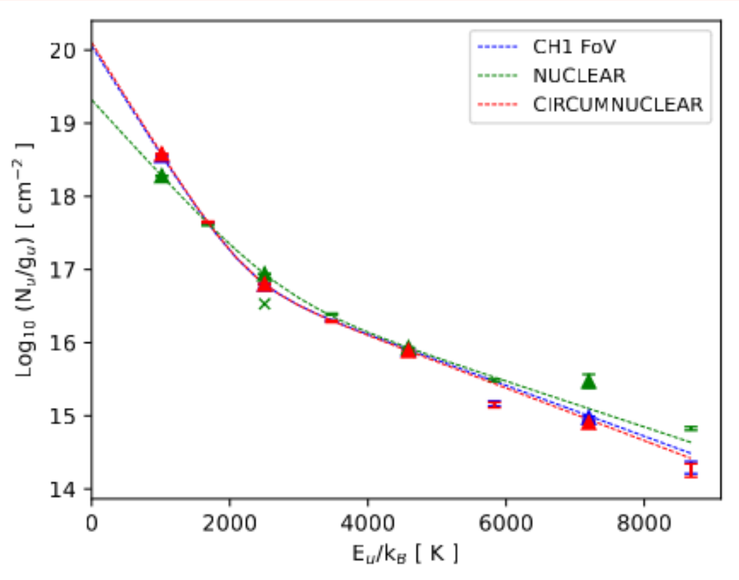

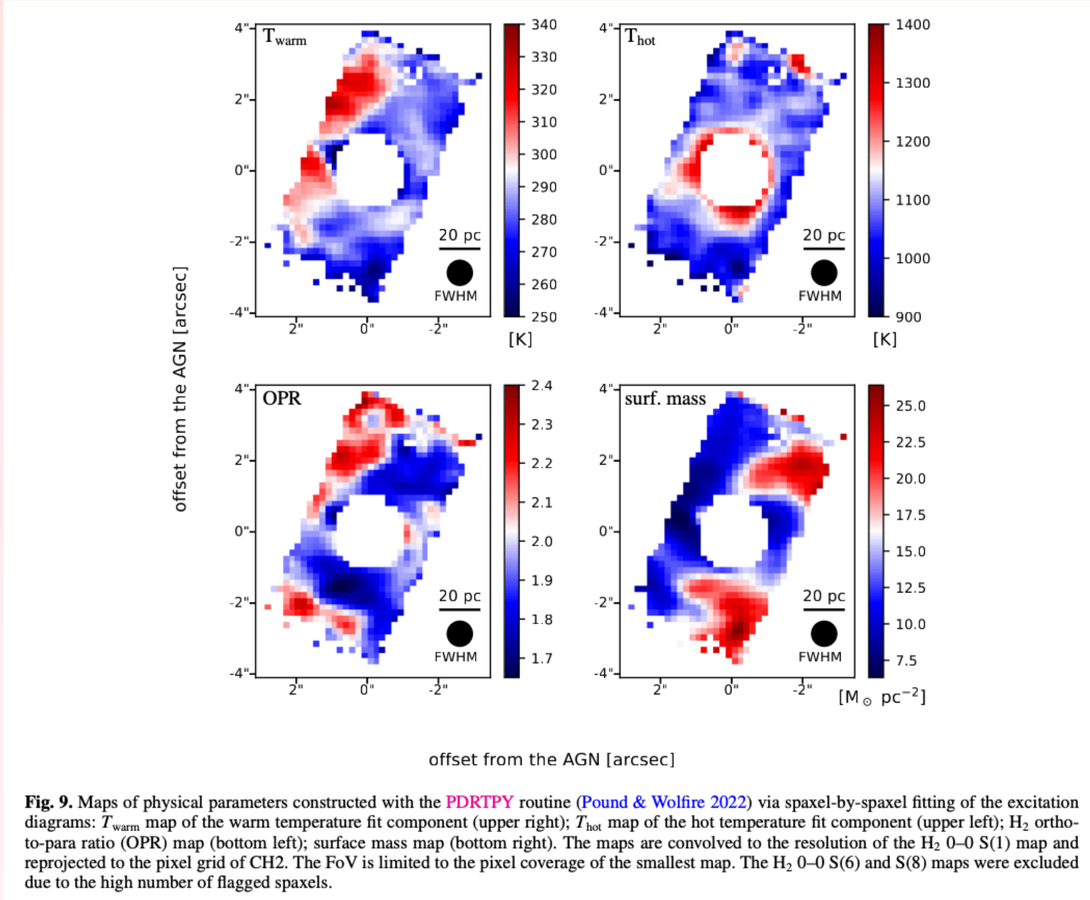

Fig. 9. Maps of physical parameters constructed with the PDRTPY routine (Pound & Wolfire 2022) via spaxel-by-spaxel fitting of the excitation diagrams: T_{warm} map of the warm temperature fit component (upper right); T_{hot} map of the hot temperature fit component (upper left); H_2 ortho-to-para ratio (OPR) map (bottom left); surface mass map (bottom right). The maps are convolved to the resolution of the H_2 0–0 S(1) map and reprojected to the pixel grid of CH2. The FoV is limited to the pixel coverage of the smallest map. The H_2 0–0 S(6) and S(8) maps were excluded due to the high number of flagged spaxels.

Evangelista et al. (2026); submitted to A&A

Backup slides

Evangelista et al. (2026); submitted to A&A

The mass of the molecular gas obtained via fit of the excitation diagram at 100 K is (9.6 ± 4) × 105 M⊙ in the inner disk, while the dynamical mass is (5 ± 0.4) × 108 M⊙ within 4" (74 pc) of the AGN.

Ratio	Full	ND	ICND	CH1	(a)	(b)
$\mathrm{Log}_{10}\left(L_{\mathrm{H_2}}/L_{24\mu\mathrm{m}}\right)$	-2.60 ± 0.04	-3.73 ± 0.04	-1.57 ± 0.04	-2.66 ± 0.04	-1.78 ± 0.04	-2.02 ± 0.04
$\mathrm{Log}_{10}\left(L_{\mathrm{H_2}}/L_{17\mu\mathrm{m}}\right)$	-2.43 ± 0.04	-3.57 ± 0.04	-1.38 ± 0.04	-2.52 ± 0.04	-1.46 ± 0.04	-1.73 ± 0.04
$\mathrm{Log}_{10}\left(L_{\mathrm{H_2}}/L_{\mathrm{PAH}_{7.7\mu\mathrm{m}}}\right)$	-0.48± 0.03	-1.05± 0.02	-0.38± 0.03	–	–	–
$\mathrm{Log}_{10}\left(L_{\mathrm{H_2}}/L_{\mathrm{X(2-10\ keV)}}\right)$	-2.36 ± 0.04	-3.29 ± 0.04	-1.89 ± 0.04	–	–	–

Table 3. Luminosity ratios between the sum of the mid-IR H_2 lines (S(1) to S(8)) and the monochromatic continuum at 24 μm, 17 μm, the $\mathrm{PAH}_{7.7\mu\mathrm{m}}$ feature, and the X-ray luminosity (2-10 keV). Extractions are from the entire FoV (Full), the ND located within an aperture of radius 2×FWHM, the ICND outside, the area covered by the FoV of CH1, as well as the Northern hotspot (a) and the Southern hotspot (b) (see Section 3.2 and Figure 3). Each H_2 line luminosity is extracted in its respective spectral MRS channel. The monochromatic continuum luminosities are extracted from the sub-cubes (see Sect. 3.5). The $\mathrm{PAH}_{7.7\mu\mathrm{m}}$ fluxes are provided by Pantoni et al. (2026). The $L_{\mathrm{X(2-10\ keV)}}$ values were obtained from Ogle et al. (2010). The spatial resolution for the $\mathrm{PAH}_{7.7\mu\mathrm{m}}$ and X-ray observations is not sufficient to perform smaller aperture extractions for the CH1, (a) and (b) regions